ESCUELA DE CONSTRUCCIÓN CIVIL
FACULTAD DE INGENIERÍA

Revista de la Construcción
Journal of Construction

Research Article

Investigation of properties of mortar containing pyrogenic silica-added supplementary cementitious materials

Gökhan Görhan[1]*, **Ahmet Mücahit Bozkurt**[2]

[1] Afyon Kocatepe University, Engineering Faculty, Department of Civil Engineering, Afyonkarahisar (Turkey), ggorhan@aku.edu.tr

[2] Afyon Kocatepe University, Engineering Faculty, Department of Civil Engineering, Afyonkarahisar (Turkey), amb0334@gmail.com

*Correspondence: ggorhan@aku.edu.tr

Received: 24.03.2021; **Accepted:** 03.03.2022; **Published:** 18.04.2022

Citation: Görhan, G. and Bozkurt, A. M. (2022). Investigation of properties of mortar containing pyrogenic silica-added supplementary cementitious materials. Revista de la Construcción. Journal of Construction, 21(1), 118-134. https://doi.org/10.7764/RDLC.21.1.118.

Abstract: this study investigated the effect of supplementary cementitious materials (SCMs) with pozzolanic nature fly-ash (FA), silica fume (SF), and ground granulated blast furnace slag (GGBFS) on the properties of cement mortar with pyrogenic silica addition. First, standard reference (SR) samples were prepared using CEM I 42.5 R-type cement. Pyrogenic silica was added to cement (0.5% by weight) to prepare another group of reference (PR) mortar samples. Cement in PR mortars was replaced with FA, SF, and GGBFS up to 10, 20, and 30%. The mortar samples were placed in 40x40x160 mm metal molds using a vibrating table. The following day the samples were removed from the molds and water cured for 7, 28, and 90 days. The results showed that increases in curing times helped improve the mechanical properties of the mortars. Moreover, the physical properties of PR mortars were affected more positively than the SR mortars. SF-substituted mortars had highest compressive strength, followed by GGBFS- and FA- substituted mortars. In conclusion, pyrogenic silica contributed to some extent to early strength, followed by a decrease.

Keywords: pyrogenic silica, mortar, cure, pozzolan, supplementary cementitious materials.

1. Introduction

The cement industry accounts for 5-7% of human-induced CO_2 emissions (Deja, Uliasz-Bochenczyk, & Mokrzycki, 2010; Šavija, Zhang, & Schlangen, 2020; Yingliang, Jingping, Zhengyu, Zhenbang, & Hui, 2020). One ton of cement is estimated to produce 0.79 tons of CO_2. Using replacement and waste materials in clinkers and raw materials can significantly reduce CO_2 emissions caused by cement manufacture (Deja et al., 2010). Therefore, pozzolanic materials have become increasingly popular in recent years (Kallel, Kallel, & Samet, 2016). Industrial waste materials with pozzolanic properties can be used in Portland cement clinkers, which is an eco-friendly option (Damtoft, Lukasik, Herfort, Sorrentino, & Gartner, 2008). Granulated blast furnace slag (GBFS) and fly ash (FA) are pozzolans commonly used in Portland cement. Granulated blast furnace slag was first used in Germany in 1865, while FA was first used at the beginning of the twentieth century (Giergiczny, 2019). Replacement materials reacting with $Ca(OH)_2$ (calcium hydroxide) in cement are also known as "supplementary cementitious materials" (SCMs). Materials containing fine particle that are by-products of silicon metal or silicon metal alloys are called “silica fume” (Erdoğan, 2003), which has high surface area. SCMs used together with silica fume form additional C-S-H in the medium, which may compensate for the slow reaction (Damtoft et al., 2008). Silica fume (SF) has a specific gravity of

2.20 to 2.30 and a specific surface area of 150,000 to 250,000 cm^2/g. SF is 100 times as thin as cement (Hatungimana, Taşköprü, İçhedef, Saç, & Yazıcı, 2019).

The most common pozzolan used in SCMs is FA, which is abundant and easy to process (Shaikh, Supit, & Sarker, 2014; Yingliang et al., 2020). Its use in concrete is commonly 20% - 25% by weight (Shaikh et al., 2014). FA is a thermal power plant waste used in cement, but it is problematic because it causes differences in compressive strength (Cho, Jung, & Choi, 2019). FA has a spherical shape and a specific gravity of 2.1 to 3.0 (Cho et al., 2019). It is gray to black, depending on the amount of unburned carbon it contains (Ahmaruzzaman, 2010). It has a particle size of 1 to 150 micrometers (Hatungimana et al., 2019).

Supplementary cementitious materials are widely used in concrete and cement. For example, blast furnace slag (BFS) and FA are suitable for partial replacement in Portland cement. They may reduce CO_2 emissions (Lothenbach, Scrivener, & Hooton, 2011), but not as much in cement manufacture. They rarely contain enough calcium to be replaced by significant quantities of limestone. One exception is BFS with around 40% CaO (Damtoft et al., 2008). Slags react pozzolanically with water because they generally contain 35%-45% CaO. Therefore, they are defined as materials with latent hydraulic properties. Their only inferiority to cement is that they have slow reaction times (Sekhar & Nayak, 2018). Slags are classified as artificial pozzolans that are metallurgical waste materials. The chemical composition and property of a slag depend on the method by which it is manufactured. BFS contains silica, calcium aluminosilicate, and basic compounds (Dorum, Koçak, Yılmaz, & Uçar, 2009). It is reported that using up to 25% BFS under different curing conditions increases compressive strength (Aldea, Young, Wang, & Shah, 2000).

Most studies on blended systems focus on the mechanical or durability properties of FA and BFS. When blending SCMs with Portland cement, normal cement hydration and SCM hydraulic reactions coincide and affect each other, causing complications. Most SCMs react more slowly than Portland cement clinker (Lothenbach et al., 2011).

In recent years, a pozzolanic material containing nano silica (NS) particles was widely used in cement and concrete to improve the durability and mechanical and physical properties of cement-based materials (Bu, Hou, Wang, & Du, 2018). NS is used to improve the microstructure of cement systems. It reacts with calcium hydroxide in the medium during hydration, resulting in C-S-H gels (Shaikh et al., 2014). In fact, recent studies about concrete utilized NS (Kong et al., 2013). Many studies address the effect of NS on cement mortar properties as it has excellent pozzolanic properties. Cement containing nano silica has a more compact structure and better mechanical properties due to nano-filling, nucleation, and pozzolanic effect (H. Liu et al., 2020). Nano silica powder or colloidal dispersions help improve the durability and mechanical properties of cement-based materials.

NS can be even more effective because it has finer particles and higher pozzolanic reactivity than SF (Kong et al., 2013). Moreover, the addition of precipitated NS helps prevent mortar chloride penetration (Kong et al., 2012) and improves water penetration resistance of concrete (Givi, Rashid, Aziz, & Salleh, 2011). Therefore, materials manufactured using nanotechnology have some unique and new functions (Ma et al., 2020). Small amounts of NS, especially at an early age (28 days), increase cement paste, mortar, and concrete strength. NS is more durable than SF. Higher strength is associated with cement hydration, reduced pores, and improved adherence between aggregate and hardened cement. NS + FA also improves the early strength of concrete (Zhang, Islam, & Peethamparan, 2012). Nanomaterials enhance the durability and early strength of modified cement-based materials (J. Wang et al., 2020).

Pyrogenic silica (PS) is a type of silica manufactured under combustion conditions with the decomposition of the precursor at high temperatures following product condensation. PS contains a different type of SiO_2 mineral (Khavryuchenko, Khavryuchenko, & Lisnyak, 2011). With low-density particles of micrometric sizes, PS is a high surface area agglomerate of amorphous silica manufactured through gas combustion. PS and NS have similar properties, but the main difference between them is that the former has higher surface area and more porous structure than the latter (Tobón, Mendoza Reales, Restrepo, Borrachero, & Payá, 2018). PS is used in different applications, including concrete admixtures (Khavryuchenko et al., 2011). Fumed silica (pyrogenic silica) is synthesized by the pyrolysis of silicon tetrachloride reacting with oxygen in a fire (Ha,

Weitzmann, & Beck, 2012). Fumed silica is a nano-sized powder that has been heterogeneously manufactured for decades. Fumed silica is used as a flow control replacement or a filler in many manufacturing processes (Veranth, Ghandehari, & Grainger, 2010). Fumed silica is composed of finely-dispersed amorphous silicon dioxide. Its surface is covered with highly reactive silanol groups for chemical reactions (Barthel, Rösch, & Weis, 1996). There is little published research about PS (Khavryuchenko et al., 2011). NS contains finer particles and thus has higher pozzolanic reaction than PS (Bu et al., 2018).

This study investigated the effect of different proportions of SCMs (FA, SF, and GGBFS) on the physical and mechanical properties of cement mortars with added pyrogenic silica.

2. Materials and methods

The cement mortars were made of CEM I 42.5 R-type cement and standard sand. Important industrial waste materials (FA, SF, and GGBFS) were added as substitutes to the cement. The fly ash (FA) was supplied by Tunçbilek Thermal Power Plant (Kütahya-Turkey) (Gümüş, 2016). The ground granulated blast furnace slag (GGBFS) and silica fume (SF) were supplied by Bolu Cement Industry Inc. (Bolu, Turkey) and Antalya Eti Electrometallurgy Facility (Antalya, Turkey), respectively. Wacker HDK® N20 was the processed pyrogenic silica of choice as a nanoscale replacement in all sample groups (Kong et al., 2012). Table 1 shows the properties of the pyrogenic silica.

Table 1. Properties of wacker HDK® N20 processed silica.

Raw material	Pyrogen hydrophilic silica
Surface area (m^2/g)	175-225
Loss on ignition	<1.5 %
Undersize	<0.03 %
Tapped density	40 g/L
pH	3.8 – 4.3

An X-ray diffraction device (Bruker, D 8 Advance) was used for XRD analysis, which detected quartz and mullite minerals in FA (Figure 1). Similar minerals in FA were reported previously (Mironyuk et al., 2019). GGBFS contained calcium silica and calcite minerals (Figure 2). However, Figure 3 shows the XRD graph of SF. Table 2 shows the results of the X-ray fluorescence (XRF) chemical analysis of the pozzolan materials. X-ray fluorescence data suggests a $(CaO+MgO)/SiO_2$ ratio higher than 1.0 in GGBFS (J. Liu, Qin, & Yu, 2020). Therefore, the GGBFS in this study met that criterion. Also, it was observed that the used SF was similar to the SF formed due to silicoferrochrome (SiFeCr) production. SiO_2 values in related SF vary between 70 – 85% (Yeğinobalı, 2011).

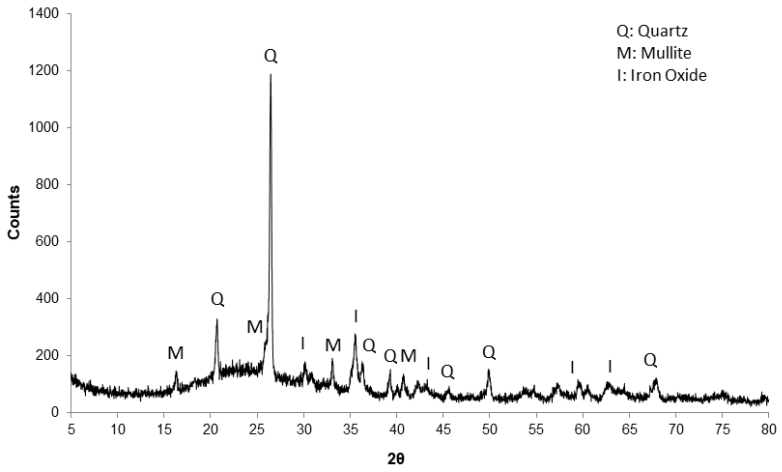

Figure 1. XRD graph of FA.

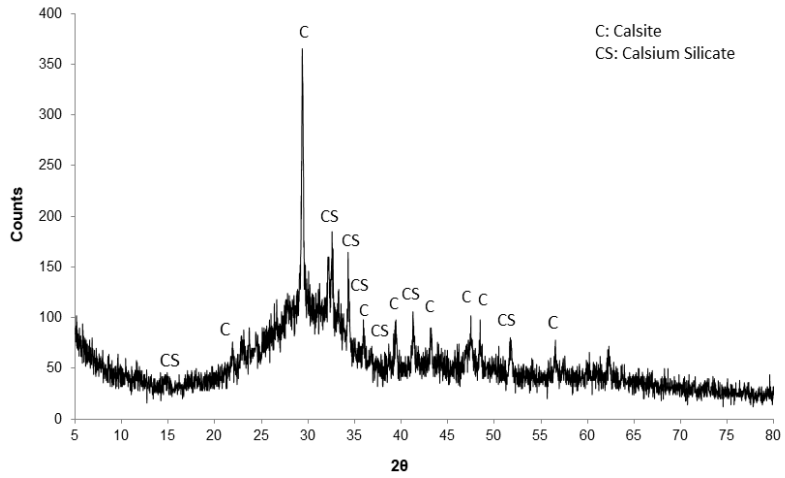

Figure 2. XRD graph of GGBFS.

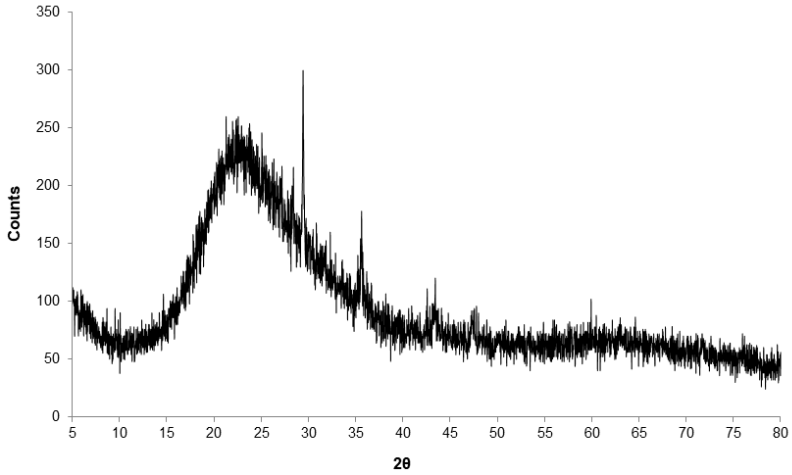

Figure 3. XRD graph of SF.

The laser particle size distribution (PSD) tests of FA and GGBFS samples were measured using a Malvern laser particle diameter analyzer. According to results d_{10}, d_{50}, and d_{90}, values of FA are 9.90, 34.01, and 127 µm, respectively. Also, d_{10}, d_{50}, and d_{90}, values of GGBFS are 2.52, 12.85, and 35.04 µm, respectively. Additionally, it is stated that SF is almost grain size smaller than 1 µm (Yeğinobalı, 2011).

Table 2. XRF analysis results.

Oxide (%)	SiO_2	Al_2O_3	Fe_2O_3	MgO	Na_2O	K_2O	SO_3	CaO	LOI	Total
GGBFS	32.22	11.67	1.55	4.19	0.48	0.95	2.22	42.64	2.26	98.18
FA (Gümüş, 2016)	55.63	21.34	9.61	4.49	0.16	1.87	0.64	3.09	1.03	97.86
SF	72.21	0.84	0.46	16.25	1.45	2.23	1.03	0.59	2.35	97.41

First, standard reference (SR) samples were prepared using CEM I 42.5 R-type cement, standard sand, and water, according to the TS EN 196-1 standard (TS EN 196-1, 2016). Then PS (0.50% by weight of cement) was added in SR mixtures. These mortars were assigned the code of "PR". The water/binder ratio was 0.5 in all mixtures.

Secondly, 10% to 30% by weight of cement was replaced by SF, GGBFS, and FA in PR mixtures, respectively. A total of 99 cement mortars (33 series and three samples in each series), including reference samples, were prepared at three curing times. Figure 4 shows the diagram for the samples.

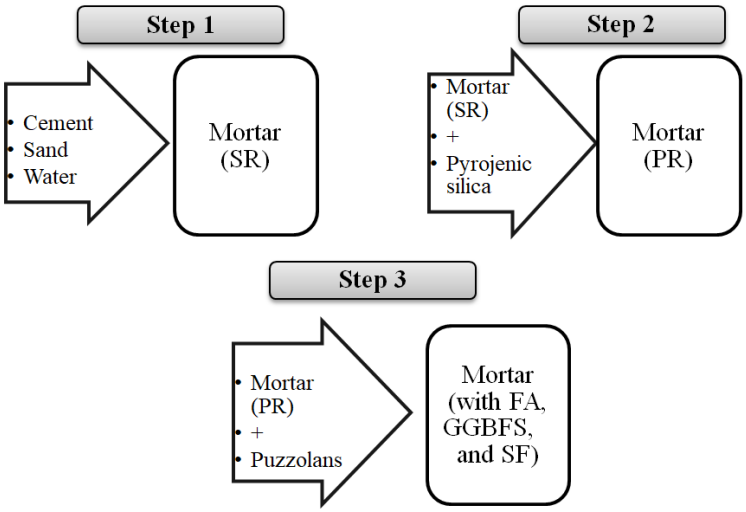

Figure 4. Mortar manufacture process.

All mixtures were prepared using a programmable automatic cement mixer (Figure 5a). First, the cement, PS, and standard sand were dry-mixed for 30 seconds according to the TS EN 196-1 standard (TS EN 196-1, 2016). Afterward, water was added to the mixture and mixed for a total of 240 seconds. The samples were placed in 40x40x160 mm metal molds using a vibrating table in the laboratory (Figure 5b). The following day, they were removed from the molds and placed in a water tank for curing for 7, 28, and 90 days. Table 3 presents the samples and mixing ratios. Abbreviations and percentages are used to refer to the mortar samples depending on the type of the pozzolanic material (SF for silica fume, GGBFS for ground granulated blast furnace slag, and FA for fly-ash) and proportion (10%, 20%, and 30%). For example, FA-20 refers to the 20% fly-ash substituted mortars.

Table 3. Samples and mixing ratios.

Code	Cement (g)	FA (g)	GGBFS (g)	SF (g)	PS (g)	Sand (g)
SR	450	-	-	-	-	1350
PR	450	-	-	-	2.25	1350
FA-10	405	45	-	-	2.25	1350
FA-20	360	90	-	-	2.25	1350
FA-30	315	135	-	-	2.25	1350
GGBFS-10	405	-	45	-	2.25	1350
GGBFS-20	360	-	90	-	2.25	1350
GGBFS-30	315	-	135	-	2.25	1350
SF-10	405	-	-	45	2.25	1350
SF-20	360	-	-	90	2.25	1350
SF-30	315	-	-	135	2.25	1350

The samples were water cured in the water tank for 7, 28, and 90 days. Afterwards, their physical properties (water absorption, apparent porosity and bulk density) were determined according to the principles of Archimedes and the TS EN 772-4 (TS EN 772-4, 2000) and TS EN 771-1 (TS EN 771-1, 2015) standards. A lab-type cement press was used to determine mechanical properties (flexural strength and compressive strength) according to the TS EN 196-1 standard (TS EN 196-1, 2016). The average of three samples from each sample group was used in the physical and mechanical tests (Figure 5c and 5d). Scanning electron microscopy (SEM) and energy-dispersive X-ray (EDS) spectroscopy analyses were performed on 90-day samples to determine their morphological characteristics and components using an SEM device LEO 1430 VP model.

(a) (b)

(c) (d)

Figure 5. The pictures of the production (a. mixer, b. produced samples, c. cured sample, d. specimens subjected to compressive test).

3. Experimental results and analysis

Apparent porosity is an important parameter because it is negatively correlated with cement paste strength (Šavija et al., 2020). The results showed that PS affected the apparent porosity of PR samples very little. This is because nanoparticles reduce free water, resulting in densely-packed particles in the matrix, while PS fills the pores and reduces porosity (Siang Ng et al., 2020; Zhu et al., 2018). PS reduced the apparent porosity of 7- and 28-day samples very little. On the other hand, 90-day samples had slightly higher apparent porosity than SR samples (Figure 6).

The apparent porosity rates varied according to the replacement type because SCMs affect the amount and type of hydrate, as well as the porosity and durability of cement systems (Lothenbach et al., 2011). Early-age SCM-Portland systems have high total porosity because the volume of hydrate products in the matrix decreases depending on the replacement ratio (Lothenbach et al., 2011). High curing times result in hydration products in cement-based mortars reducing porosity rates (Figure 6).

The highest rate of porosity was caused by FA, followed by GGBFS and SF. The 28- and 90-day pozzolan-substituted samples had lower porosity in the matrix than SR samples. The higher the FA, the more varied the porosity. Higher rates of replacement only increased the porosity of 7-day samples (Figure 6a). However, there was no correlation between the replacement ratios and porosity in 28- and 90-day samples (Figures 6b and 6c). The higher the replacement ratio, the higher the porosity of 7-day GGBFS samples. The higher the replacement ratio, the lower the porosity of 28-day GGBFS samples. The 28- and 90-day GGBFS samples had lower apparent porosity than SR and PR samples.

BFS can be used to manufacture impervious concrete (Binici, Kaplan, Temiz, & Görür, 2008) and ternary mixtures of Portland cement, BFS and limestone (Díaz, Izquierdo, Mejía De Gutiérrez, & Gordillo, 2013), but NS and BFS reduce the porosity and increase the cement matrix density (M. Liu, Zhou, Zhang, Yang, & Cheng, 2016). All SF sample groups had the lowest porosity, which decreased with the increase in the replacement ratio. However, SF-20 and SF-30 samples had similar porosity rates. The 90-day samples had the lowest apparent porosity ranging from 6.8% to 11.1%.

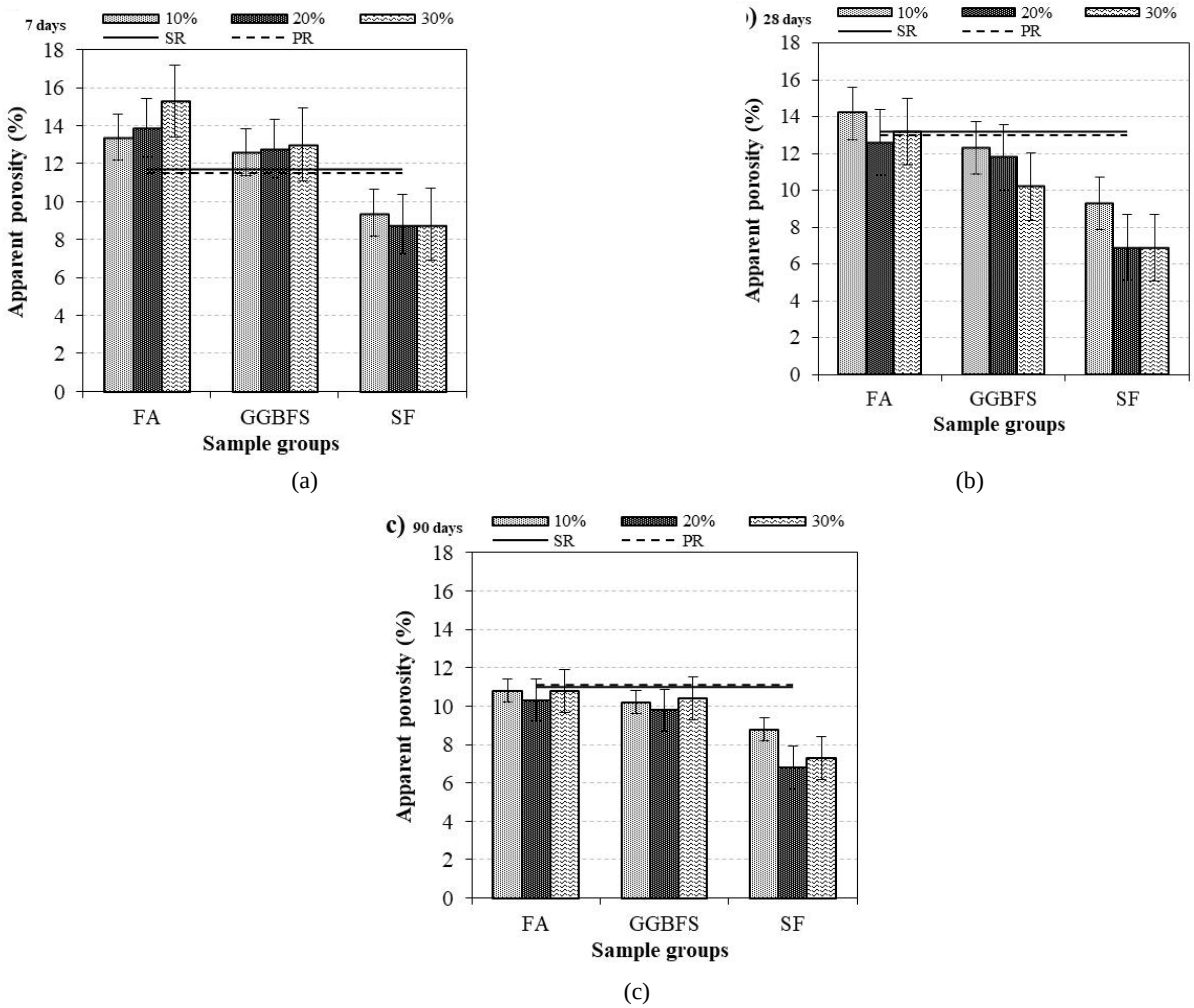

Figure 6. Apparent porosity rates.

PS affected the absorption rates slightly. Of PS mortars, SF samples had the lowest water absorption rates at all curing times. The higher the replacement ratio of SF, the better the internal structure (Hatungimana et al., 2019), resulting in reduced water absorption rates. The higher the replacement of SF, the lower the water absorption rates in 28-day samples. However, the higher the FA replacement ratio, the higher the water absorption rates due to little pozzolanic reaction (Hatungimana et al., 2019). This is consistent with our results. However, they also found that longer curing times led to lower water absorption rates.

The increase in replacement ratios slightly increased the water absorption of 7-day GGBFS and FA samples. Of all samples, FA samples had the highest water absorption rates (Figure 7a). In all sample groups, the samples cured for a long time had lower water absorption rates than those cured for a short time (Figure 7c). All pozzolan-substituted samples had lower water absorption rates than PR and SR samples. FA and SF samples had the highest and lowest water absorption rates at all curing times, respectively. This result shows that the replacement ratios changed the water absorption rates. All 90-day pozzolan-substituted samples had water absorption rates of 4.1% to 5.1%, while SR and PR samples had water absorption rates of 5.1% and 5.2%, respectively.

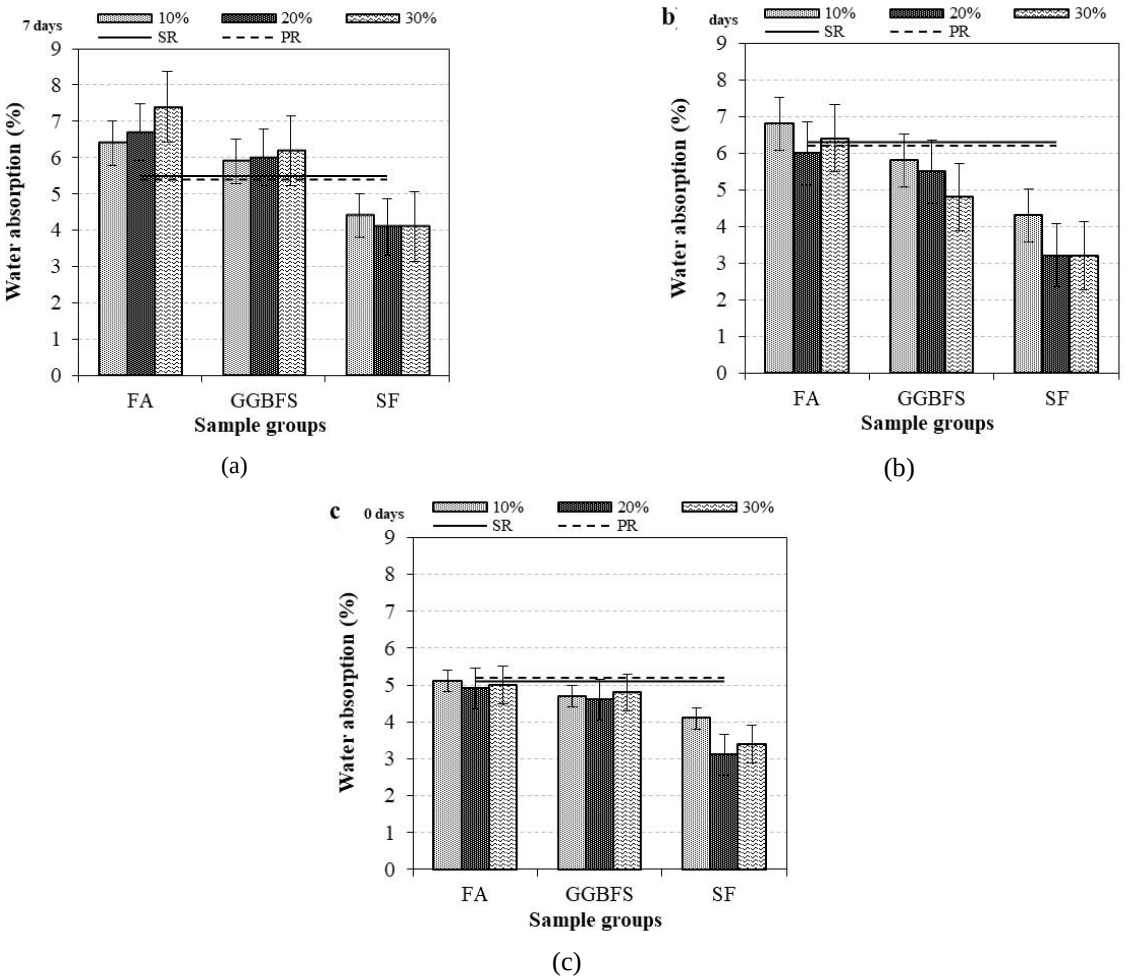

Figure 7. Water absorption rates by weight.

The curing times changed the bulk density of SR and PR samples. Compared to 7- and 28-day SR samples, the bulk density of 7- and 28-day PR samples increased, but the bulk density of 90-day samples decreased. PS is a good pozzolanic material because it has small particles with high packing ability (Bu et al., 2018). Therefore, we can state that PS contributes to bulk density in the early stages. It is also reported that PS helps improve density (Kong et al., 2012).

The higher the replacement ratios, the lower the bulk density of 7-day FA and GGBFS samples. However, the replacement ratios did not affect the bulk density of SF samples. Higher replacement ratios led to higher bulk density of 28-day GGBFS and SF samples. What is more, 28-day SF-20 samples had higher bulk density than 28-day GGBFS-20 samples. Of 90-day mortars, SF-20 samples had the highest bulk density (2184.70 kg/m^3) at all curing times and for all material groups. An increasing trend was observed in SF-substituted samples up to 20% substitution and a decreasing trend was seen for 30% substitution samples. SF samples had the highest bulk density rates at all curing times. This may be because SF fills the voids between hydrated cement particles formed by free water, resulting in a denser porous microstructure in cement (Hatungimana et al., 2019). Our results corroborate this. Higher replacement ratios resulted in lower bulk density in FA samples but not in SF and GGBFS samples. FA samples had bulk density of 2054.3 kg/m^3 to 2129.1 kg/m^3. GGBFS samples had bulk density of 2116.5 kg/m^3 to 2150.5 kg/m^3. SF samples had bulk density of 2151.2 kg/m^3 to 2184.7 kg/m^3 (Figure 8).

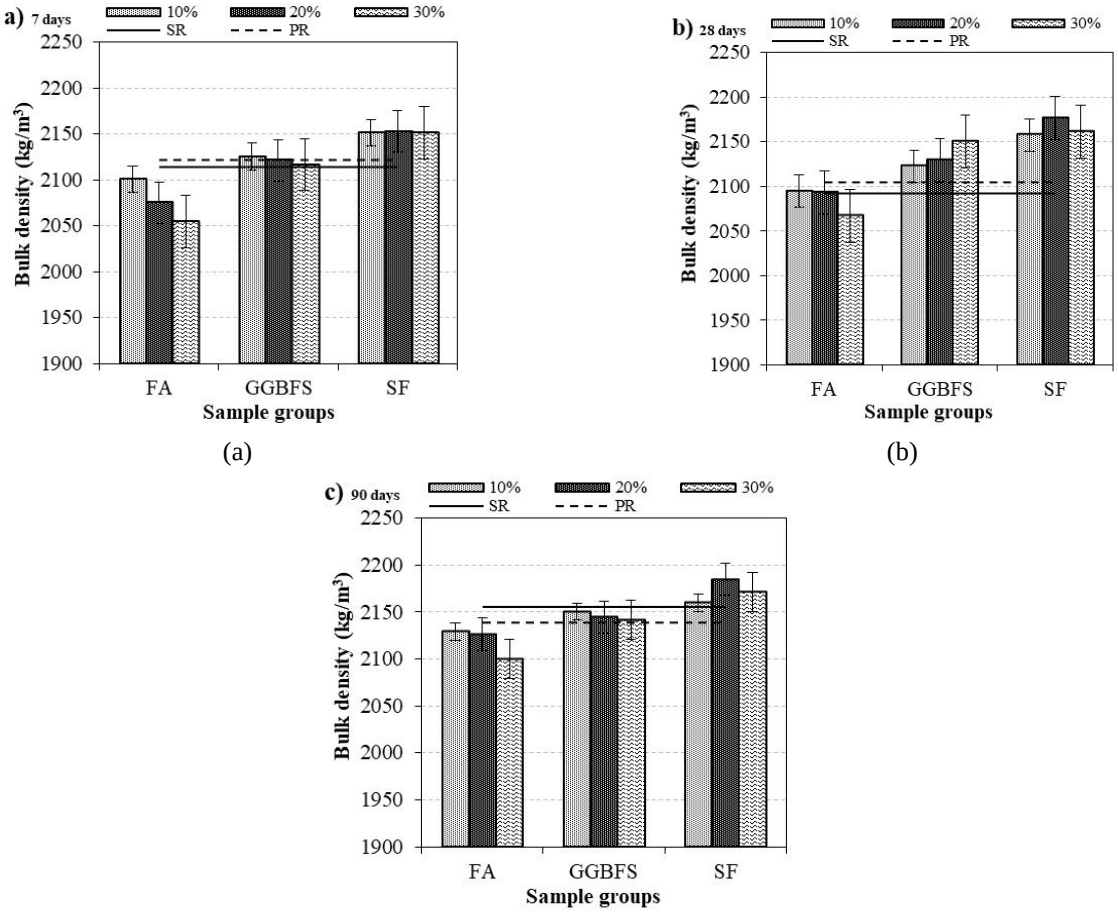

Figure 8. Bulk density rates.

Flexural strength is an important mechanical property in building materials. There was a positive correlation between curing times and flexural strength, but not in all sample groups (Figure 9). Of SR mortars, 28-day samples had the highest flexural strength. The 7- and 28-day PS samples had higher flexural strength than SR samples, whereas 90-day PS samples had lower flexural strength than SR samples. It is reported that 7-day PS samples have higher flexural and compressive strength than control samples (Bu et al., 2018). Therefore, the increase in curing time increased the flexural strength of PS samples to a certain point, after which it decreased the flexural strength.

The increase in replacement ratios caused no change in the flexural strength of 7-day FA samples. However, the increase in replacement ratios led to a change in the flexural strength of 7-day GGBFS and SF samples. The 7-day PR samples had almost the same flexural strength as 7-day SF samples. The 28-day SR and PR samples had similar flexural strength values. The 28-day FA and GGBFS samples also had similar flexural strength values. Of 28-day mortars, SF samples had the lowest flexural strength. There was no linear relationship between replacement ratios and flexural strength in 7- and 28-day pozzolan-substituted samples. However, the higher the replacement ratios, the higher the flexural strength of 90-day pozzolan substituted samples, especially GGBFS-30. The high lime content of blast furnace slag allows for semi-hydraulic reactions, even in the absence of Portland cement (Skibsted & Snellings, 2019). The higher the replacement ratios, the higher the flexural strength values of GGBFS and SF samples. The 7-, 28-, and 90-day samples had flexural strength of 6.8 MPa to 9.6 MPa, 7.9 MPa to 10.3 MPa, and 7.8 MPa – 10.2 MPa, respectively (Figure 9).

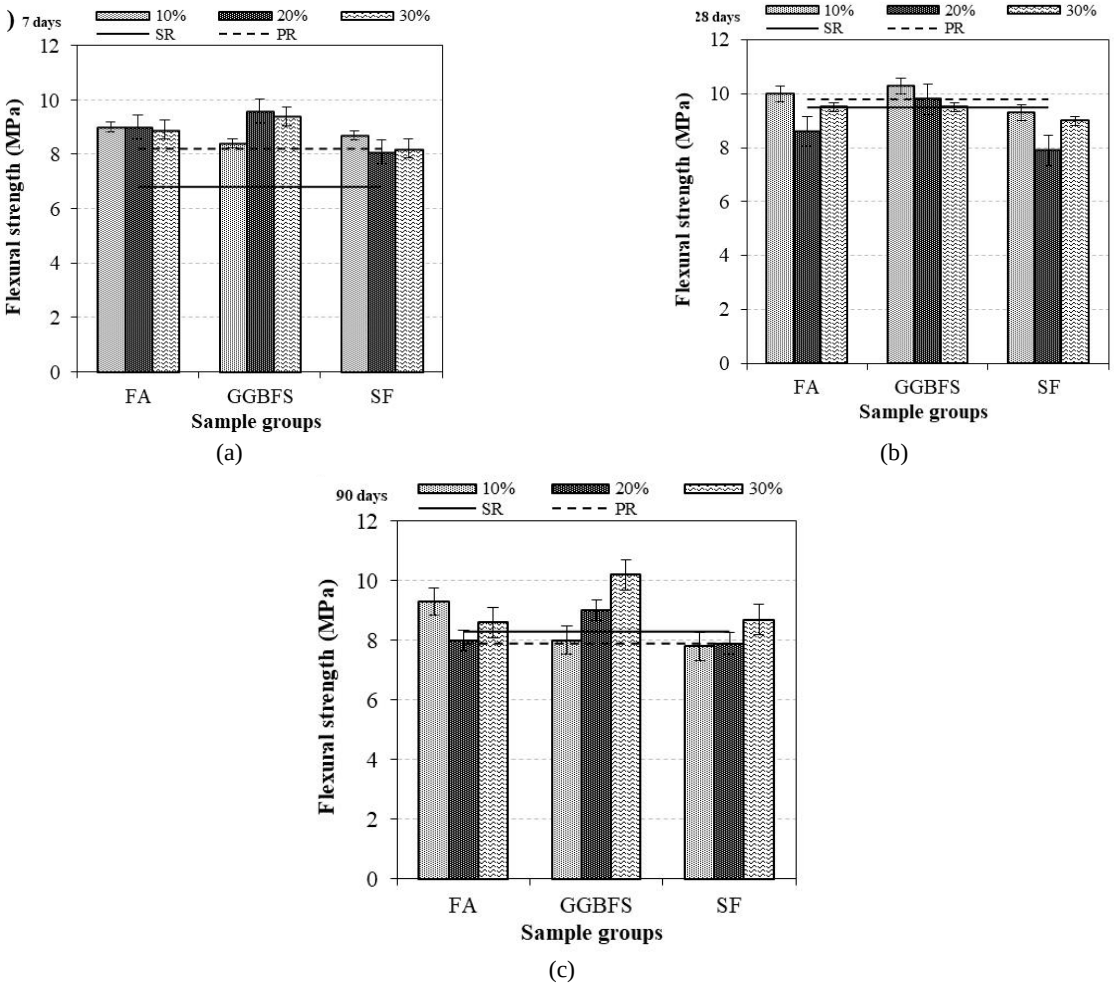

Figure 9. Flexural strength values.

Nano-silica, with similar properties to pyrogenic silica, has accelerating effects because it rapidly consumes the calcium ions in the paste (Kong et al., 2013). PS accelerates the setting times of low-reactive cement, providing significant contributions to early strength (Bost, Regnier, & Horgnies, 2016). The 28-day PR samples had higher compressive strength than 28-day SR samples. PS affects the hydration reaction of cement to a certain extent and the cross-linking of hydration products (Li, Wang, & Wu, 2020). However, PS triggers $Ca(OH)_2$ consumption, and therefore, has a more significant effect on concrete strength than on cement strength (Zhu et al., 2018). Thus, PS may have a limited impact on the compressive strength of cement mortars (Figure 10). Studies about the effects of nanoparticles on cement composites do not specify the amount of nanoparticles that should be used to improve the properties of cementitious materials with fly-ash (Siang Ng et al., 2020). They also argue that PS has no significant effect on cement compressive strength at low temperatures (Bu et al., 2018). The 90-day FA samples had lower compressive strength than SR and PR samples (Figure 10c), while 7- and 28-day FA samples had lower compressive strength than SR samples (Figures 10a and 10b).

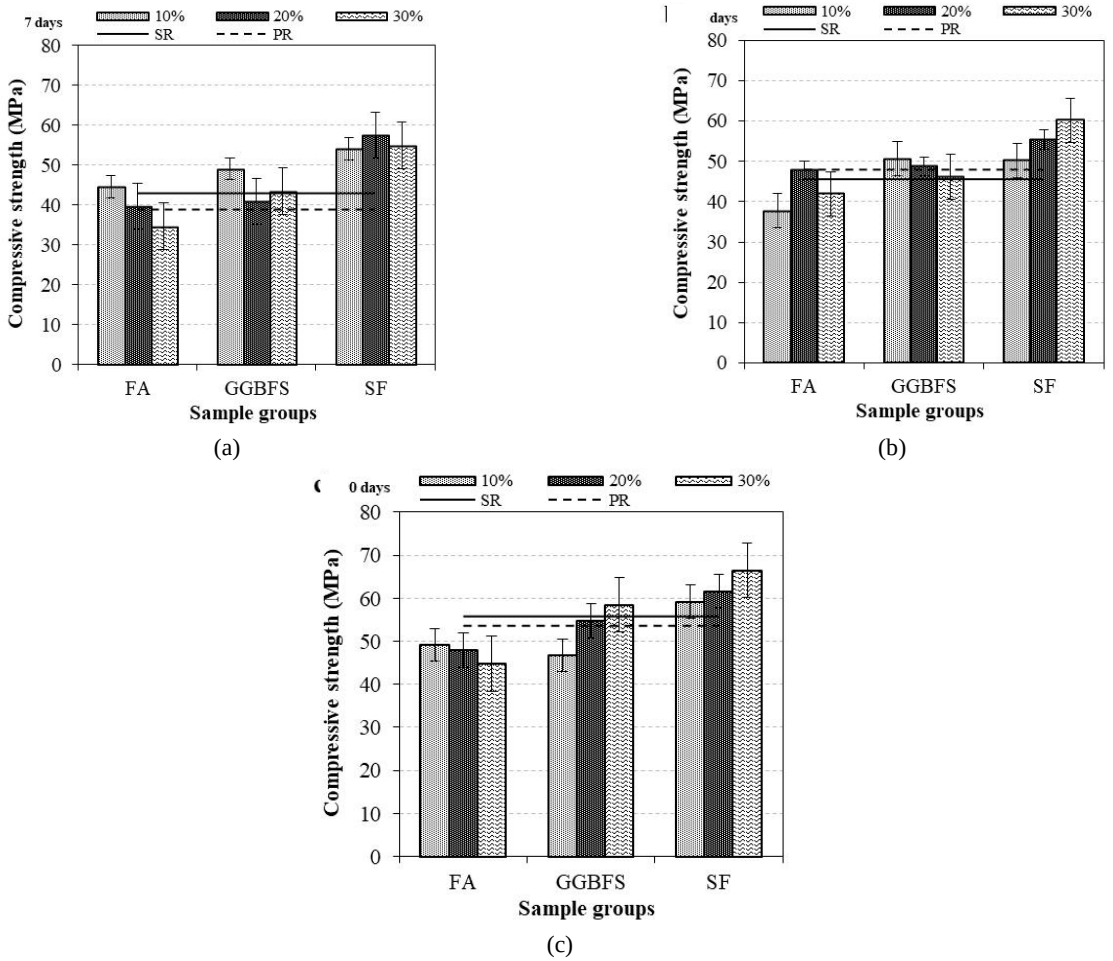

Figure 10. Compressive strength values.

High rates of fly ash substitution result in low compressive strength in conventional Portland cement. FA also causes prolonged hydration because it reacts slowly at room temperature. Therefore, it takes FA at least seven days to react effectively (Yingliang et al., 2020). Even FA from the same power plant has variable effects on samples (T. Wang, Ishida, Gu, & Luan, 2020). In light of this information, FA samples had lower compressive strength than GGBFS and SF samples at all curing times. It is reported that it takes FA at least 60 and 28 days, respectively, to improve the compressive and flexural strength of mortars (Siang Ng et al., 2020). In another study, it was stated that lower compressive strength values were obtained in fly ash-substituted samples compared to silica fume-substituted and reference samples (Hatungimana et al., 2019). In the samples with 25% fly ash substitution, the 28-day compressive strength values of the fly ash mortars with different chemical contents varied between 41.1 and 51.5 MPa (Cho et al., 2019), and it was observed that they were compatible with the values obtained in this study. We also found that 90-day FA samples had compressive strength of 34.7 MPa to 49.2 MPa (Figure 10). The 7-day FA-20 and -30 samples had lower compressive strength values than SR samples. In the literature, it was determined that 7-day FA-5 cement samples had slightly higher, but 28-day FA-5 cement samples had slightly lower compressive strength values than reference samples (Mironyuk et al., 2019). In the 7-, 28-, and 90-day samples with up to 45% of FA replacement, lower compressive strength values were found compared to reference samples at all curing times (Elmrabet, El Harfi, & El Youbi, 2019), which is consistent with our results. At this point, the pozzolanic activity of FA used in cement systems depends significantly on its chemical composition (Cho et al., 2019).

The greatest difference between flexural and compressive strength was observed in SF samples, which had the highest compressive strength at all replacement ratios. SF substitution leads to extra C-S-H products in the cement matrix, resulting

in increased compressive strength (Hatungimana et al., 2019), which is consistent with our results. Compared to SR and PR samples, 7-day SF samples had significantly different compressive strength values, while 28- and 90-day SF samples had slightly higher compressive strength values than reference samples. Higher SF replacement ratios led to higher compressive strength in samples subjected to the same curing times. The 90-day SF-30 samples had the highest compressive strength (66.5 MPa) (Figure 10c).

GGBFS, which exhibits erratic behavior in cement mortar, was used as an SCM in Portland cement in recent years (Gao, Meng, Yang, Tang, & Lv, 2019). Therefore, it was reported that the glassy content of BFS affects compressive strength due to its latent hydraulic feature, but that the glassy content of 88% or greater had no significant impact on compressive strength (J. Liu et al., 2020). NS-3 cement mortars were found to have higher compressive strength than BFS-40 and untreated samples (M. Liu et al., 2016). Our results showed that PS and GGBFS mortars yielded variable outcomes. The 7-day GGBFS samples and 28-day GGBFS-10 and -20 samples had higher compressive strength values than PR mortars. The 7-day GGBFS-10 and -30 samples and all 28-day GGBFS samples had higher compressive strength values than SR mortars. Studies reported that 7- and 28-day BFS-20 and -30 mortars had lower compressive strength values than reference samples (Dorum et al., 2009; Yingliang et al., 2020).

Therefore, our results suggest that PS and GGBFS samples had a better reaction increasing at all curing times. The 28-day samples had a compressive strength of 37.7 MPa to 60.2 MPa. The 90-day samples had a compressive strength of 44.8 MPa to 66.5 MPa. Of 90-day mortars, the higher the replacement ratio, the lower the compressive strength in FA samples, while higher replacement ratio led to higher compressive strength in GGBFS and SF samples. GGBFS-20 and -30 samples and all SF samples had higher compressive strength than SR and PR samples (Figure 10c). However, it was reported that PS substitution up to 10% affected the compressive strength of 7- and 28-day cement mortars less than NS (Tobón et al., 2018).

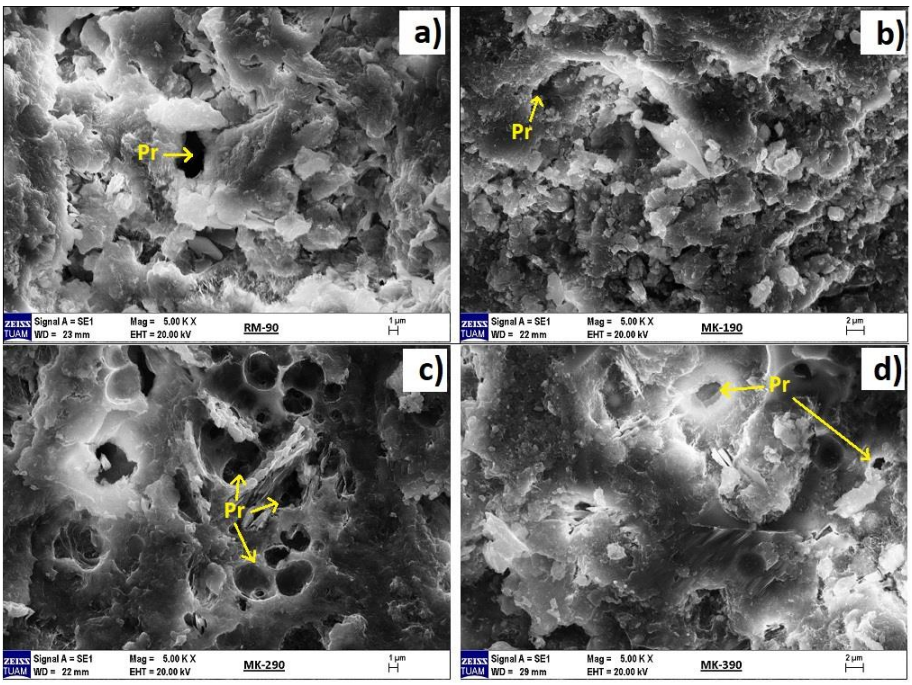

Figure 11. SEM analyses of mortars.

The SEM images indicated no major morphological difference (Figures 11 and 12). When the surface morphology of the samples was examined, it was observed that the pozzolans substituted for cement decreased the pore (Pr) sizes compared to the reference samples. While the pore size was ~ 5 µm in the reference samples, the size of the open pores decreased to ~ 1.4 µm with the replacement additives made to the cement. However, no significant cracks were observed in the surface morphology.

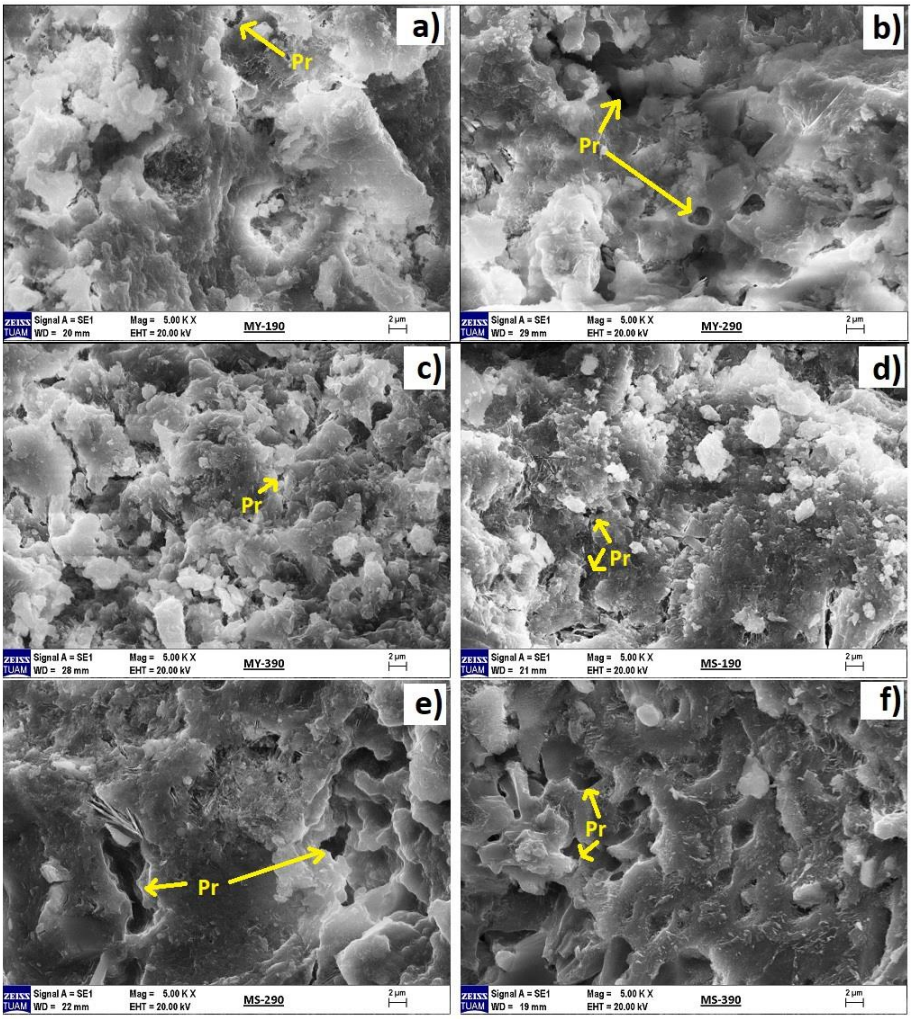

Figure 12. SEM analyses of mortars.

Spatial EDS analysis was performed on 90-day samples. SEM-EDS analysis of some samples is given in Figure 13. The analysis results obtained from the samples are given in Table 4. It was determined that the pozzolans increased Al_2O_3 values in the material compared to the reference samples. At the same time, depending on the MgO content in the SF, MgO content was determined in the SF samples in SEM-EDS analysis.

Table 4. SEM-EDS analysis results.

Oxide (%)	SR	FA-10	FA-20	FA-30	GGBFS-10	GGBFS-20	GGBFS-30	SF-10	SF-20	SF-30
SiO_2	57.26	54.64	37.94	50.54	38.11	43.73	38.18	38.87	48.67	66.32
Al_2O_3	2.91	10.19	5.76	6.01	3.65	4.23	4.72	6.05	6.41	3.09
CaO	39.83	35.17	56.30	43.46	58.24	52.04	57.11	53.17	41.78	28.22
MgO	-	-	-	-	-	-	-	1.90	3.15	2.37

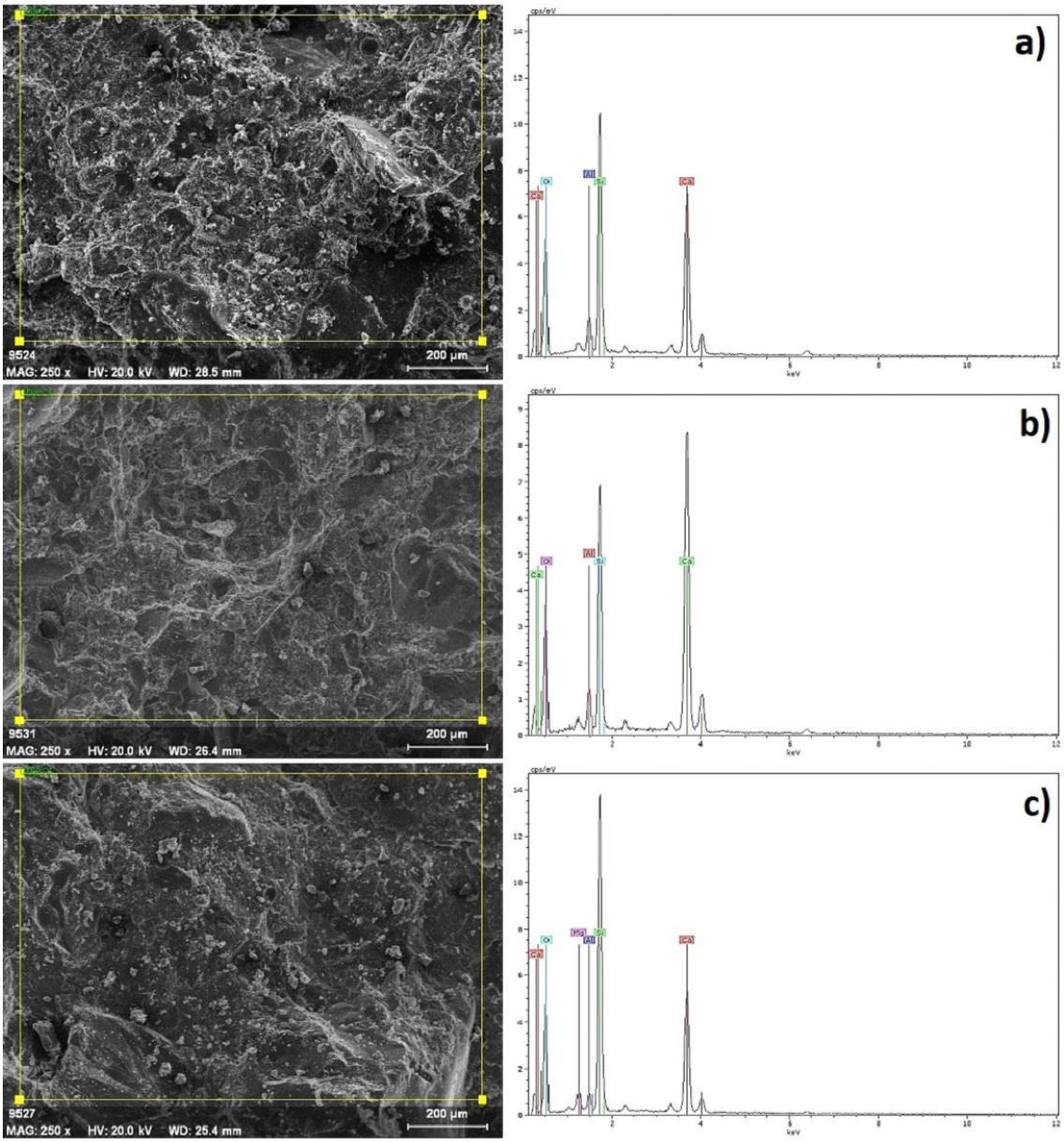

Figure 13. SEM-EDS analyses of mortars (a. FA-30, b. GGBFS-30, c. SF-30).

4. Conclusions

This study investigated the effect of three pozzolanic materials (FA, SF, and GGBFS) on pyrogenic siliceous mortar properties. According to the results:

1. In the early stages (7- and 28- day), PS samples had slightly lower apparent porosity and water absorption. Therefore, PS contributed to bulk density in the early stages;
2. While FA samples had the highest porosity and water absorption in all sample groups, SF samples had the lowest porosity and water absorption rates. The relative values tend to decrease with increasing SF ratio. However, SF samples had the highest bulk density in all sample groups;

3. The positive contribution of PS to the flexural strengths decreased with increasing curing time. In addition, despite the increase in the replacement ratios, variable results were obtained for the flexural strengths. Increasing substitution rates increased the strengths only in GGBFS specimens cured for 90 days;
4. FA samples had the lowest compressive strength values with increasing replacement ratio in the sample groups. However, the highest compressive strength values were obtained in SF samples;
5. SF reacted better than GGBFS and FA and had higher compressive strength than reference mortars at replacement ratios and curing times;
6. As a result, PS contributed to early strength, followed by a decrease.

Author contributions: Gökhan GÖRHAN: Conceptualization, Methodology, Writing- Original draft,
Ahmet Mücahit BOZKURT: Visualization, Investigation.

Funding: Afyon Kocatepe University, The Scientific Research Projects Coordination Unit, Project No: 17.FEN.BİL.39.

Acknowledgments: The authors would like to thank Afyon Kocatepe University, the Scientific Research Projects Coordination Unit (Project No: 17.FEN.BİL.39), for the financial support for this study.

Conflicts of interest: Not Applicable.

References

Ahmaruzzaman, M. (2010). A review on the utilization of fly ash. Progress in Energy and Combustion Science, 36(3), 327–363. https://doi.org/10.1016/j.pecs.2009.11.003

Aldea, C. M., Young, F., Wang, K., & Shah, S. P. (2000). Effects of curing conditions on properties of concrete using slag replacement. Cement and Concrete Research, 30(3), 465–472. https://doi.org/10.1016/S0008-8846(00)00200-3

Barthel, H., Rösch, L., & Weis, J. (1996). Fumed silica - production, properties, and applications. In Organosilicon Chemistry II: From Molecules to Materials (pp. 761–778). Weinheim, Germany: Wiley-VCH Verlag GmbH. https://doi.org/10.1002/9783527619894.ch91

Binici, H., Kaplan, H., Temiz, H., & Görür, E. B. (2008). Some durability properties of ground blast furnace slag and ground basaltic pumice concretes. Journal of Engineering Sciences, 14(3), 309–317. Retrieved from http://dergipark.gov.tr/download/article-file/190984

Bost, P., Regnier, M., & Horgnies, M. (2016). Comparison of the accelerating effect of various additions on the early hydration of Portland cement. Construction and Building Materials, 113, 290–296. https://doi.org/10.1016/j.conbuildmat.2016.03.052

Bu, Y., Hou, X., Wang, C., & Du, J. (2018). Effect of colloidal nanosilica on early-age compressive strength of oil well cement stone at low temperature. Construction and Building Materials, 171, 690–696. https://doi.org/10.1016/j.conbuildmat.2018.03.220

Cho, Y. K., Jung, S. H., & Choi, Y. C. (2019). Effects of chemical composition of fly ash on compressive strength of fly ash cement mortar. Construction and Building Materials, 204, 255–264. https://doi.org/10.1016/j.conbuildmat.2019.01.208

Damtoft, J. S., Lukasik, J., Herfort, D., Sorrentino, D., & Gartner, E. M. (2008). Sustainable development and climate change initiatives. Cement and Concrete Research, 38(2), 115–127. https://doi.org/10.1016/j.cemconres.2007.09.008

Deja, J., Uliasz-Bochenczyk, A., & Mokrzycki, E. (2010). CO2 emissions from Polish cement industry. International Journal of Greenhouse Gas Control, 4(4), 583–588. https://doi.org/10.1016/j.ijggc.2010.02.002

Díaz, J. E., Izquierdo, S. R., Mejía De Gutiérrez, R., & Gordillo, M. (2013). Ternary mixture of portland cement, blast furnace slag and limestone: mechanical strength and durability. Revista de La Construcción. Journal of Construction, 12(3), 55–62.

Dorum, A., Koçak, Y., Yılmaz, B., & Uçar, A. (2009). The effects of blast furnace slag on the cement surface properties and hydration. Journal of Science and Technology of Dumlupinar University, 19, 47–58.

Elmrabet, R., El Harfi, A., & El Youbi, M. S. (2019). Study of properties of fly ash cements. Materials Today: Proceedings, 13, 850–856. Elsevier Ltd. https://doi.org/10.1016/j.matpr.2019.04.048

Erdoğan, T. Y. (2003). Beton. Metu Press - TURKEY.

Gao, D., Meng, Y., Yang, L., Tang, J., & Lv, M. (2019). Effect of ground granulated blast furnace slag on the properties of calcium sulfoaluminate cement. Construction and Building Materials, 227, 116665. https://doi.org/10.1016/j.conbuildmat.2019.08.046

Giergiczny, Z. (2019). Fly ash and slag. Cement and Concrete Research, 124, 105826. https://doi.org/10.1016/j.cemconres.2019.105826

Givi, A. N., Rashid, S. A., Aziz, F. N. A., & Salleh, M. A. M. (2011). Investigations on the development of the permeability properties of binary blended concrete with nano-SiO2 particles. Journal of Composite Materials, 45(19), 1931–1938. https://doi.org/10.1177/0021998310389091

Gümüş, A. (2016). Effect of thermal curing process on geopolymer concrete properties. Afyon Kocatepe University, M.Sc. Thesis, Institute of Science and Technology, Department of Civil Engineering, Afyonkarahisar- TURKEY.

Ha, S. W., Weitzmann, M. N., & Beck, G. R. (2012). Dental and skeletal applications of silica-based nanomaterials. In Nanobiomaterials in Clinical Dentistry (pp. 69–91). Elsevier Inc. https://doi.org/10.1016/B978-1-4557-3127-5.00004-0

Hatungimana, D., Taşköprü, C., İçhedef, M., Saç, M. M., & Yazıcı, Ş. (2019). Compressive strength, water absorption, water sorptivity and surface radon exhalation rate of silica fume and fly ash based mortar. Journal of Building Engineering, 23, 369–376. https://doi.org/10.1016/j.jobe.2019.01.011

Kallel, T., Kallel, A., & Samet, B. (2016). Durability of mortars made with sand washing waste. Construction and Building Materials, 122, 728–735. https://doi.org/10.1016/j.conbuildmat.2016.06.086

Khavryuchenko, V. D., Khavryuchenko, O. V., & Lisnyak, V. V. (2011). Formation of pyrogenic silica: Spectroscopic and quantum chemical insight. Critical Reviews in Solid State and Materials Sciences, 36(2), 47–65. https://doi.org/10.1080/10408436.2011.572741

Kong, D., Du, X., Wei, S., Zhang, H., Yang, Y., & Shah, S. P. (2012). Influence of nano-silica agglomeration on microstructure and properties of the hardened cement-based materials. Construction and Building Materials, 37, 707–715. https://doi.org/10.1016/j.conbuildmat.2012.08.006

Kong, D., Su, Y., Du, X., Yang, Y., Wei, S., & Shah, S. P. (2013). Influence of nano-silica agglomeration on fresh properties of cement pastes. Construction and Building Materials, 43, 557–562. https://doi.org/10.1016/j.conbuildmat.2013.02.066

Li, Z., Wang, Y., & Wu, Y. (2020). Nano fumed silica particles on cement properties. IOP Conference Series: Earth and Environmental Science, 525, 012149. https://doi.org/10.1088/1755-1315/525/1/012149

Liu, H., Jin, J., Yu, Y., Liu, H., Liu, S., Shen, J., … Ji, H. (2020). Influence of halloysite nanotube on hydration products and mechanical properties of oil well cement slurries with nano-silica. Construction and Building Materials, 247, 118545. https://doi.org/10.1016/j.conbuildmat.2020.118545

Liu, J., Qin, Q., & Yu, Q. (2020). The effect of size distribution of slag particles obtained in dry granulation on blast furnace slag cement strength. Powder Technology, 362, 32–36. https://doi.org/10.1016/j.powtec.2019.11.115

Liu, M., Zhou, Z., Zhang, X., Yang, X., & Cheng, X. (2016). The synergistic effect of nano-silica with blast furnace slag in cement based materials. Construction and Building Materials, 126, 624–631. https://doi.org/10.1016/j.conbuildmat.2016.09.078

Lothenbach, B., Scrivener, K., & Hooton, R. D. (2011). Supplementary cementitious materials. Cement and Concrete Research, 41(12), 1244–1256. https://doi.org/10.1016/j.cemconres.2010.12.001

Ma, C., He, J., Qin, T., Long, G., Du, Y., & Xie, Y. (2020). A comparison of the influence of micro- and nano-silica on hydration kinetics of Portland cement under different temperatures. Construction and Building Materials, 248, 118670. https://doi.org/10.1016/j.conbuildmat.2020.118670

Mironyuk, I., Tatarchuk, T., Paliychuk, N., Heviuk, I., Horpynko, A., Yarema, O., & Mykytyn, I. (2019). Effect of surface-modified fly ash on compressive strength of cement mortar. Materials Today: Proceedings, 35, 534–537. https://doi.org/10.1016/j.matpr.2019.10.016

Šavija, B., Zhang, H., & Schlangen, E. (2020). Micromechanical testing and modelling of blast furnace slag cement pastes. Construction and Building Materials, 239, 117841. https://doi.org/10.1016/j.conbuildmat.2019.117841

Sekhar, D. C., & Nayak, S. (2018). Utilization of granulated blast furnace slag and cement in the manufacture of compressed stabilized earth blocks. Construction and Building Materials, 166, 531–536. https://doi.org/10.1016/j.conbuildmat.2018.01.125

Shaikh, F. U. A., Supit, S. W. M., & Sarker, P. K. (2014). A study on the effect of nano silica on compressive strength of high volume fly ash mortars and concretes. Materials and Design, 60, 433–442. https://doi.org/10.1016/j.matdes.2014.04.025

Siang Ng, D., Paul, S. C., Anggraini, V., Kong, S. Y., Qureshi, T. S., Rodriguez, C. R., … Šavija, B. (2020). Influence of SiO2, TiO2 and Fe2O3 nanoparticles on the properties of fly ash blended cement mortars. Construction and Building Materials, 258, 119627. https://doi.org/10.1016/j.conbuildmat.2020.119627

Skibsted, J., & Snellings, R. (2019). Reactivity of supplementary cementitious materials (SCMs) in cement blends. Cement and Concrete Research, 124, 105799. https://doi.org/10.1016/j.cemconres.2019.105799

Tobón, J. I., Mendoza Reales, O., Restrepo, O. J., Borrachero, M. V., & Payá, J. (2018). Effect of pyrogenic silica and nanosilica on portland cement matrices. Journal of Materials in Civil Engineering, 30(10), 04018266. https://doi.org/10.1061/(asce)mt.1943-5533.0002482

TS EN 196-1. (2016). Methods of testing cement - Part 1: Determination of strength. Ankara-TURKEY.

TS EN 771-1. (2015). Specification for masonry units - Part 1: Clay masonry units. Ankara-TURKEY.

TS EN 772-4. (2000). Methods of test for masonry units - Part 4: Determination of real and bulk density and of total and open porosity for natural stone masonry units. Ankara-TURKEY.

Veranth, J. M., Ghandehari, H., & Grainger, D. W. (2010). Nanoparticles in the Lung. In Comprehensive Toxicology, Second Edition (Vol. 8, pp. 453–475). Elsevier Inc. https://doi.org/10.1016/B978-0-08-046884-6.00928-3

Wang, J., Cheng, Y., Yuan, L., Xu, D., Du, P., Hou, P., … Wang, Y. (2020). Effect of nano-silica on chemical and volume shrinkage of cement-based composites. Construction and Building Materials, 247, 118529. https://doi.org/10.1016/j.conbuildmat.2020.118529

Wang, T., Ishida, T., Gu, R., & Luan, Y. (2020). Experimental investigation of pozzolanic reaction and curing temperature-dependence of low-calcium fly ash in cement system and Ca-Si-Al element distribution of fly ash-blended cement paste. Construction and Building Materials, 267, 121012. https://doi.org/10.1016/j.conbuildmat.2020.121012

Yeğinobalı, A. (2011). Silis dumanı ve çimento ile betonda kullanımı (7th ed.). Ankara: TÇMB/AR-GE Enstitüsü, TURKEY.

Yingliang, Z., Jingping, Q., Zhengyu, M. A., Zhenbang, G., & Hui, L. (2020). Effect of superfine blast furnace slags on the binary cement containing high-volume fly ash. Powder Technology, 375, 539–548. https://doi.org/10.1016/j.powtec.2020.07.094

Zhang, M. H., Islam, J., & Peethamparan, S. (2012). Use of nano-silica to increase early strength and reduce setting time of concretes with high volumes of slag. Cement and Concrete Composites, 34(5), 650–662. https://doi.org/10.1016/j.cemconcomp.2012.02.005

Zhu, N., Jin, F., Kong, X., Xu, Y., Zhou, J., Wang, B., & Wu, H. (2018). Interface and anti-corrosion properties of sea-sand concrete with fumed silica. Construction and Building Materials, 188, 1085–1091. https://doi.org/10.1016/j.conbuildmat.2018.08.040